Available online at www.sciencedirect.com

ScienceDirect

Current Opinion in Structural Biology

Combining single-molecule and structural studies reveals protein and DNA conformations and assemblies that govern DNA mismatch repair

Dorothy A. Erie[1] and Keith R. Weninger[2]

DNA mismatch repair (MMR) requires coordinated sequential actions of multiple proteins during a window of time after the replication apparatus makes an error and before the newly synthesized DNA undergoes chromosome compaction and/or methylation of dGATC sites in some γ-proteobacteria. In this review, we focus on the steps carried out by MutS and MutL homologs that initiate repair. We connect new structural data to early and recent single-molecule FRET and atomic force microscopy (AFM) studies to reveal insights into how signaling within the MMR cascade connects MutS homolog recognition of a mismatch to downstream repair. We present unified models of MMR initiation that account for the differences in the strand discrimination signals between methyl- and non-methyl-directed MMR.

Addresses
[1] Department of Chemistry and Lineberger Comprehensive Cancer Center, University of North Carolina, Chapel Hill, NC 27599, USA
[2] Department of Physics, North Carolina State University, Raleigh, NC 27695, USA

Corresponding author: Erie, Dorothy A. (derie@unc.edu)

Current Opinion in Structural Biology 2024, **89**:102917

This review comes from a themed issue on **Protein Nucleic Acid Interactions (2024)**

Edited by **Junji Iwahara** and **David C. Williams Jr.**

For complete overview of the section, please refer the article collection - Protein Nucleic Acid Interactions (2024)

Available online 10 September 2024

https://doi.org/10.1016/j.sbi.2024.102917

Introduction

Maintenance of the integrity of the DNA genome is key to survival in all organisms, and the DNA mismatch repair (MMR) system plays a major role in mutation avoidance. MMR proteins identify and correct errors made by DNA polymerase during replication [1–5]. MMR is initiated by the conserved MutS and MutL homologues, which both harbor ATPase and DNA binding domains. In MMR, MutS and MutL homologs function as a homodimers in prokaryotes and heterodimers in eukaryotes [1,6,7]. Prokaryotic MutS homodimers can associate to form tetramers [8–10]; however, mutations that eliminate tetramerization have minimal effect on MMR [6,7,11] but appear to play a role in anti-recombination *in vivo* [7]. Eukaryotes contain multiple MutS and MutL homologs, of which MSH2-MSH6 (MutSα) and MLH1-PMS2 (Mlh1-Pms1 in yeast) (MutLα) are the primary homologs in MMR, with MSH2-MSH3 (MutSβ) and MLH1-MLH3 (Mutγ) playing secondary roles [1]. In this review, we focus on MMR studies of prokaryotic MutS and MutL and eukaryotic MutSα and MutLα (collectively noted as MutS(α) and MutL(α)). MutS(α) searches for replication errors, and after recognizing an error, it undergoes ATP-dependent conformational changes that lead to the recruitment of one or more MutL(α) to form MutS(α)-MutL(α)-DNA (SL) complexes [1,2,4,12–24]. These SL complexes signal the downstream events that lead to repair. In humans, mutations in the genes that code for MutSα or MutLα cause Lynch syndrome, the most common hereditary cancers [3,25–28].

MMR is unique among DNA repair pathways because the repair machinery must discriminate between the original DNA and the daughter strand that contains the replication error. A cascade of signaling by MutS(α) and MutL(α) leads to a nick(s) specifically in the daughter strand, from which excision commences. After excision, DNA polymerase fills the gap, correcting the error. Organisms employ two distinct mechanisms to generate daughter-strand nicks. In methyl-directed MMR, which occurs in *Escherichia coli* and some γ-proteobacteria [29], MutL activates the latent endonuclease activity of MutH to nick the transiently unmethylated dGATC sites in the daughter strand; whereas, in non-methyl-directed MMR, which is utilized by all eukaryotes and most bacteria, MutL(α) contains a latent endonuclease activity that is activated by PCNA in eukaryotes or β-clamp in prokaryotes to specifically nick the daughter strand [30–32]. These differences in the strand discrimination signals result in MMR signaling pathways in methyl- and non-methyl-directed MMR that diverge after the ATP- and mismatch-dependent recruitment of MutL(α) by MutS(α). In this review, we connect new structural data to early and recent single-molecule studies to reveal insights into how signaling within the MMR

cascade links MutS(α) recognition of a mismatch to downstream repair.

MutS dynamically interconverts between open and closed states

On mismatch DNA, MutS(α) forms a theta-like structure, with two channels formed by the ATPase (Domains V) and clamp (Domains IV) domains on the ends and Domains I (one of which interacts specifically with the mismatch) in the middle, separating the two channels (Figure 1e, right) [33–36]. The DNA binding site is in the channel formed by four mobile domains (Domains I and IV on each subunit). These domains make predominately nonspecific interactions with DNA, and the only specific contacts to the mismatch base are with a conserved Phe and Glu from one Domain I (Subunit A in prokaryotes and MSH6 in eukaryotes) [33–36]. In eukaryotes, interaction between Domains I of MSH2 and MSH6 increase mismatch binding affinity [37]. As discussed below, ATP binding drives large conformational changes in the four mobile domains that regulate repair signaling.

Single-molecule FRET (smFRET) studies of the relative positions of the Domains I of *Thermus aquaticus* (*Taq*) MutS in the presence of nucleotide but absence of DNA revealed two main classes of states, one with high FRET and the other with lower FRET [15] (Figure 1). The diverse array of MutS conformations recently observed with crystallography and cryo-electron microscopy (cryo-EM) in the absence of DNA [38,39] provide a structural framework to interpret these smFRET results. In the crystal structures of mismatch-bound MutS(α) and the cryo-EM structure of ADP:ATP-bound DNA-free *E. coli* MutS [38], Domains I are closed, in a position that would produce high FRET (Figure 1e, left). In contrast, Domains I have moved apart in the crystal structures of *Neisseria gonorrhoeae* (*Ngo*) MutS without DNA [39], and several cryo-EM structures of *E. coli* MutS lack resolution of one of Domains I, suggesting they are mobile. These distributions of conformations are consistent with the distribution of low FRET states seen in smFRET. These structures also show the clamp domains (IV) in open and closed states, suggesting that MutS can dynamically convert between states in which Domains I and IV are open and closed. Similarly, recent cryo-EM structures of MutSβ show multiple conformations of both Domains I and IV [40] suggesting that the dynamic nature of these domains may be universal for MutS homologs.

During scanning DNA for a mismatch, MutS adopts two classes of conformations

When MutS is scanning homoduplex DNA with both ends blocked, smFRET shows two dominant states, similar to those for free MutS [15] (Figure 1). Interestingly, on unblocked DNA where a free end allows a diffusing MutS to slide off, only the high FRET

Figure 1

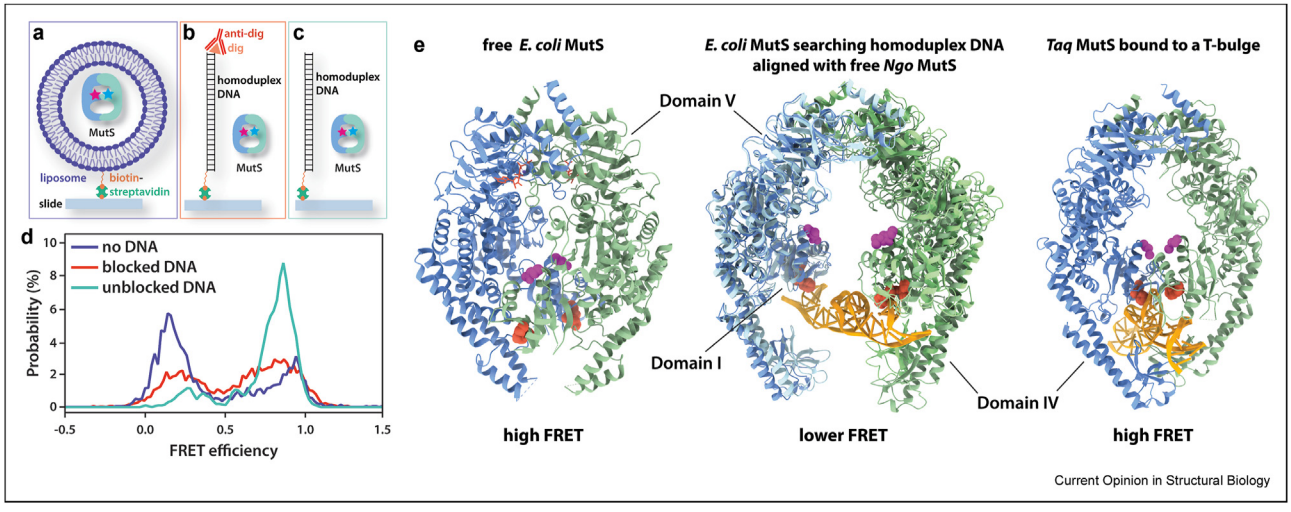

Free MutS and MutS scanning DNA exhibit conformational states with the Domains I and IV in open and closed conformations. (**a–c**) Cartoons showing the smFRET experiments used to monitor conformational changes in *Taq* MutS Domains I in the absence of DNA in liposomes attached to the surface (**a**) and in the presence of homoduplex DNA attached to the surface, with the free end blocked by anti-digoxigenin (**b**) or unblocked (**c**). (**d**) Histograms of distribution of smFRET values for free MutS (blue) and MutS bound to blocked (red) and unblocked (cyan) homoduplex DNA in the presence of ATP (adapted from Ref. [15]). (**e**) cryo-EM and crystal structures of ADP:ATP-bound DNA-free *E. coli* MutS (left; PDB: 7OU4), *E. coli* MutS-homoduplex overlayed with DNA-free *Ngo* MutS (middle; *Ngo* MutS shown in darker color; PDBs: 7AI5, 5X9W), and *Taq* MutS bound to a T-bulge (right; PDB: 1EWQ). The orange spheres show the conserved Phe and Glu, and the magenta spheres show the residues on *E. coli* MutS that align with *Taq* MutS-M88C (*E.coli*: Q86) to which the dyes are attached for smFRET. Domains I, IV, and V represent the domains that can interact with the mismatch, the clamp domains, and the ATPase domains, respectively. The more open states (middle) will generate lower FRET distributions than the closed states (left and right) and could represent conformations in the lower and higher FRET peaks in **d**.

population (closed) is observed, suggesting that it is diffusing along the DNA more slowly than the open state (low FRET). Examination of recent cryo-EM and crystal structures and molecular dynamics (MD) simulations, coupled with early atomic force microscopy (AFM) studies of MutS interacting with homoduplex DNA suggests that these low and high FRET populations may represent MutS bound to straight DNA (open) and to bent DNA (closed), respectively [41–46]. MD studies find that MutS-homoduplex DNA complexes dynamically convert between bent and straight DNA states accompanied by movement of Domains I and IV of subunits A and B, respectively; however, MutS appears unable to diffuse without distorting the DNA [41,42]. Early AFM experiments that showed MutS induces bending on homoduplex DNA, with the conserved Glu promoting bending, support the suggestion that MutS distorts the DNA during searching [43,44]. In the cryo-EM structure of MutS-homoduplex DNA complexes, the DNA was stretched across the grid resulting in MutS interacting with straight DNA in a conformation that is dramatically different from the mismatch bound state or the MD conformations [41,42], but it is remarkably similar to the *Ngo* MutS structure without DNA [39] (Figure 1e, middle). In this cryo-EM structure, Domains I and IV are open and all interactions appear to be with the backbone (no groove interactions). Single-molecule tracking and polarization studies of *E. coli* MutS and *Saccharomyces cerevisiae* (*Sc*) MutSα on homoduplex DNA suggest that MutS(α) tracks the groove while scanning DNA [45,46]. Furthermore, MutS(α) must interact with the groove to recognize the mismatch. These observations suggest that *E. coli* MutS-homoduplex DNA structure (Figure 1e, middle) may not represent a productive searching state. It could, however, represent the fast-diffusing low FRET state seen in the smFRET studies on blocked DNA (Figure 1).

After mismatch recognition, MutS undergoes ATP-dependent conformational changes that allow recruitment of MutL and/or mobile clamp formation

During scanning, MutS(α) likely induces a smooth bend in the DNA [41,43,44], and upon interaction with a mismatched base, the smooth bend converts to a kink, with the mismatched base rotated toward the minor groove, stacking with the conserved Phe and making an H-bond to the Glu. In the absence of ATP, the MutS-mismatch complex dynamically interconverts between states with different extents of DNA bending, with the ability to adopt relatively unbent states correlated with repair efficiency [43,44,47,48]. smFRET of *Taq* proteins (Figure 2a–c; [17,49]) coupled with cryo-EM and X-ray structural studies of *E. coli* MutS and MutL [16–18,20,49–54] suggest that in the presence of ATP, repair signaling proceeds by a coordinated series of conformational changes involving DNA bending/unbending, crossing of the clamp domains, and sequential movement of Domains I away from the DNA (Figure 2). Once the first Domain I (subunit B) opens, MutL can interact with the complex to activate downstream repair processes. If MutL does not arrive in time, the mismatch binding Domain I (subunit A) also opens, allowing the formation of a mobile clamp that can move away from the mismatch. In the absence of ATP hydrolysis, this mobile clamp conformation cannot rebind the mismatch, consistent with the mismatch-binding Domain I being disengaged from the DNA; however, ATP hydrolysis drives conformational changes that re-engage the mismatch-binding domain with DNA and allow the clamp to rebind the mismatch [49]. MutL can bind either clamp conformation and stop or dramatically slow MutS [16,20,49].

Quantitative analysis of kinetics of *Taq* MutS smFRET transitions provides an estimation of the free energy landscape that illustrates the downhill path leading to the first mobile clamp state (Figure 2c, State 4) [17,49]. In the absence of ATP hydrolysis, this state is much more stable (lower free energy) than the mismatch-bound intermediate (Figure 2c, State 3). ATP hydrolysis drives a conformational change, re-engaging the mismatch binding domain with the DNA and raising the energy of the clamp (Figure 2c, State 5) such that it can rebind the mismatch. Because MutL can stop MutS clamp movement, repetitive rebinding of the mismatch by MutS should increase the probability that SL complexes, which initiate repair, localize near the mismatch [49,55].

MutL(α) dimerizes via the C-terminal domains, which are linked to the N-terminal domains by flexible linker arms (ranging from ~25aa to ~200aa depending on subunit and organism) [50,51,53,54,56–58] (Figure 3a). The N-terminal domains contain ATPase and DNA binding activities [59–61], and the C-terminal domain (of PMS2/Pms1 in eukaryotes) harbors the PCNA (β-clamp in prokaryotes) binding and endonuclease sites in non-methyl-directed MMR organisms [30–32,51,54,62–64], and in eukaryotes the conserved C-terminal residues of Mlh1 make up part of the endonuclease site [54] (Figure 3). The N-terminal domain of MutL(α) interacts with MutS(α) when one of the DNA binding and adjacent connector domains opens and exposes the MutL(α) binding site (Figure 2) [17,18,52,65]. In *E. coli* MutL, which does not have endonuclease activity, ATP promotes dimerization of the N-terminal domains [59]. In eukaryotes, ATP drives asymmetric condensation of the MLH1 and PMS2 linker arms, bringing the N- and C-terminal domains together [56] (Figure 3a). These conformational changes bring the DNA binding domains and the endonuclease site in close proximity [56], suggesting that the ATP-induced changes in MutL(α) orient the DNA in the endonuclease site for cleavage [55]. Consistent with this suggestion, AlphaFold2 [66–68]

Figure 2

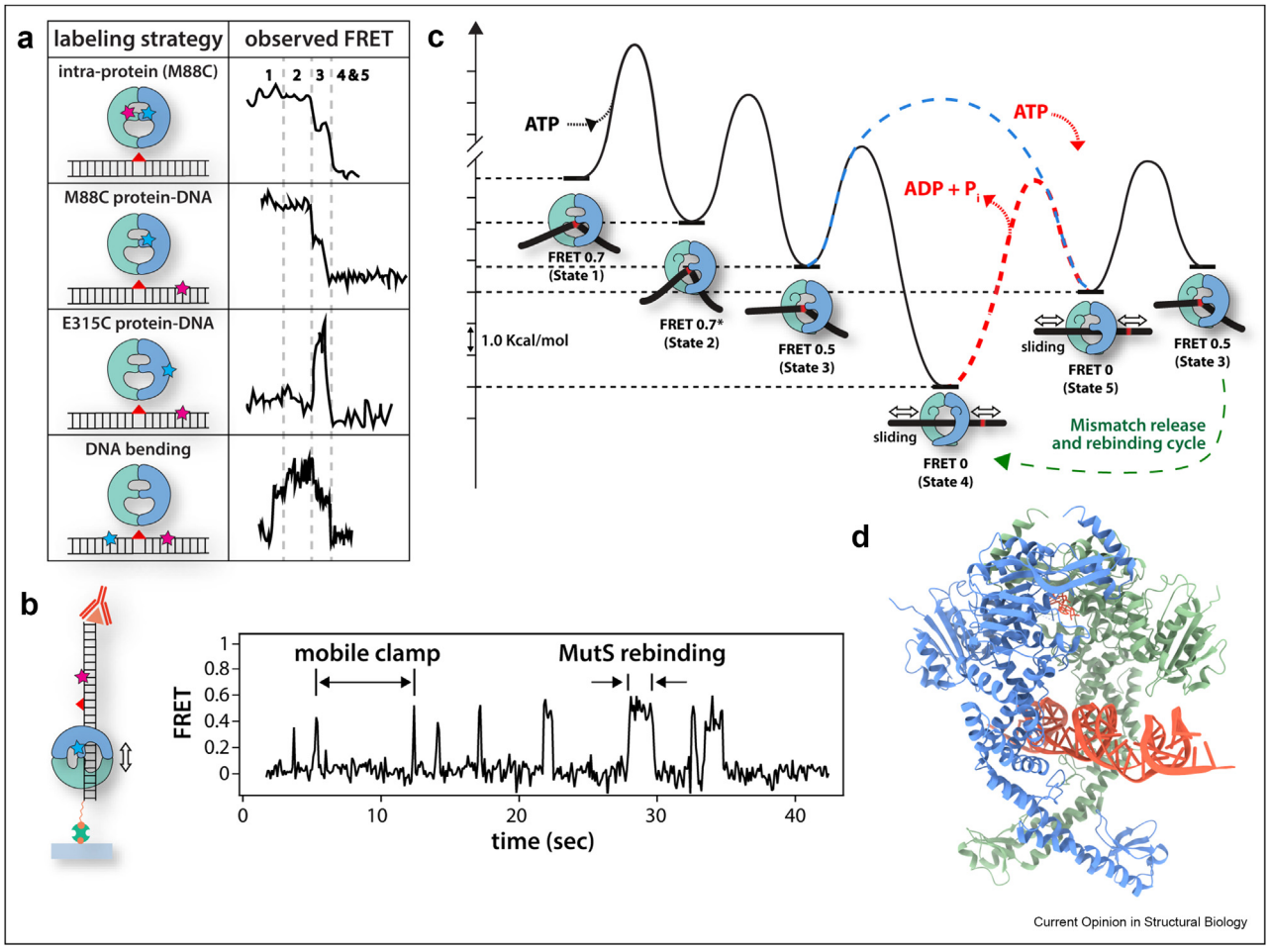

smFRET studies reveal the coordinated conformational changes in Taq MutS Domains I and the mismatch DNA as MutS transits from mismatch recognition to mobile clamp and back. (**a**) Table showing the FRET labeling strategies (left column; donor: blue star, acceptor: red star) and example FRET traces of the corresponding cooridinated transitions (right column). The mismatch is denoted as a red mark on the DNA, MutS subunits A and B are colored blue and green, respectively. The vertical dotted lines on the smFRET traces denote transitions that were identified both by their position in the pathway and their kinetics (adapted from Ref. [17]), and the numbers above the transitions correspond to the states shown in **c**. These labeling schemes (from top to bottom) are used to monitor the relative positions of *i*) Domains I, *ii*) Domain I and DNA, *iii*) the "immobile" E315 and DNA to assess DNA movement, and *iv*) DNA flanking the mismatch to assess DNA bending. (**b**) Example smFRET trace showing MutS repetitively transitioning between a mobile clamp (0 FRET) and mismatch bound state (0.5 FRET), with a cartoon of the experiment on left. (**c**) Energetic pathway based on smFRET kinetics of MutS transitioning from mismatch to mobile clamp and back to the mismatch. The FRET value shown for each state corresponds to MutS-M88C-DNA FRET. State 1: mismatch recognition with both Domains I binding and bending the DNA at the mismatch; State 2: conformational change with increased DNA bending but no discernable changes in protein-protein or protein-DNA FRET; State 3: additional conformational change at the mismatch, in which Domain I of Subunit B disengages DNA, with decreased DNA bending and lower protein-protein and Domain I-DNA FRET, but higher MutS-E315C-DNA FRET; State 4: low energy "initial" mobile clamp state with both Domains I open and with very low (~0) protein-protein FRET and a protein-DNA FRET of 0; State 5: ATP hydrolysis driven higher energy mobile clamp state (protein-DNA FRET 0), with mismatch binding Domain I (Subunit A) interacting with the DNA such that MutS can rebind mismatch into conformational State 3 (green dashed arrow). Panels **b** and **c** are adapted from Ref. [49]. (**d**) cryo-EM *E. coli* MutS:MutL-N-terminal domain structure (PDB:7AIB) showing clamp domains crossed. MutL is hidden for clarity.

models of *Taq* MutL (Figure 3b), which has relatively short linker arms (residues 314–341), shows collapsed structures with interactions between the N- and C-terminal domains. Electrostatic maps of these models reveal a positively charged “pore” between the N- and C-terminal domains adjacent to the endonuclease site that could represent the general location of DNA (Figure 3b, right).

Similar to *Taq*, smFRET studies with *E. coli* proteins showed that a single MutL can stop (or greatly slow) a MutS mobile clamp [20,69]. Interestingly, these studies also found that MutL could leave MutS and rapidly diffuse along the DNA, sometimes passing a DNA-bound MutS. This fast-scanning MutL can interact with MutH and facilitate its localization of a hemi-methylated dGATC site. These studies also showed

Figure 3

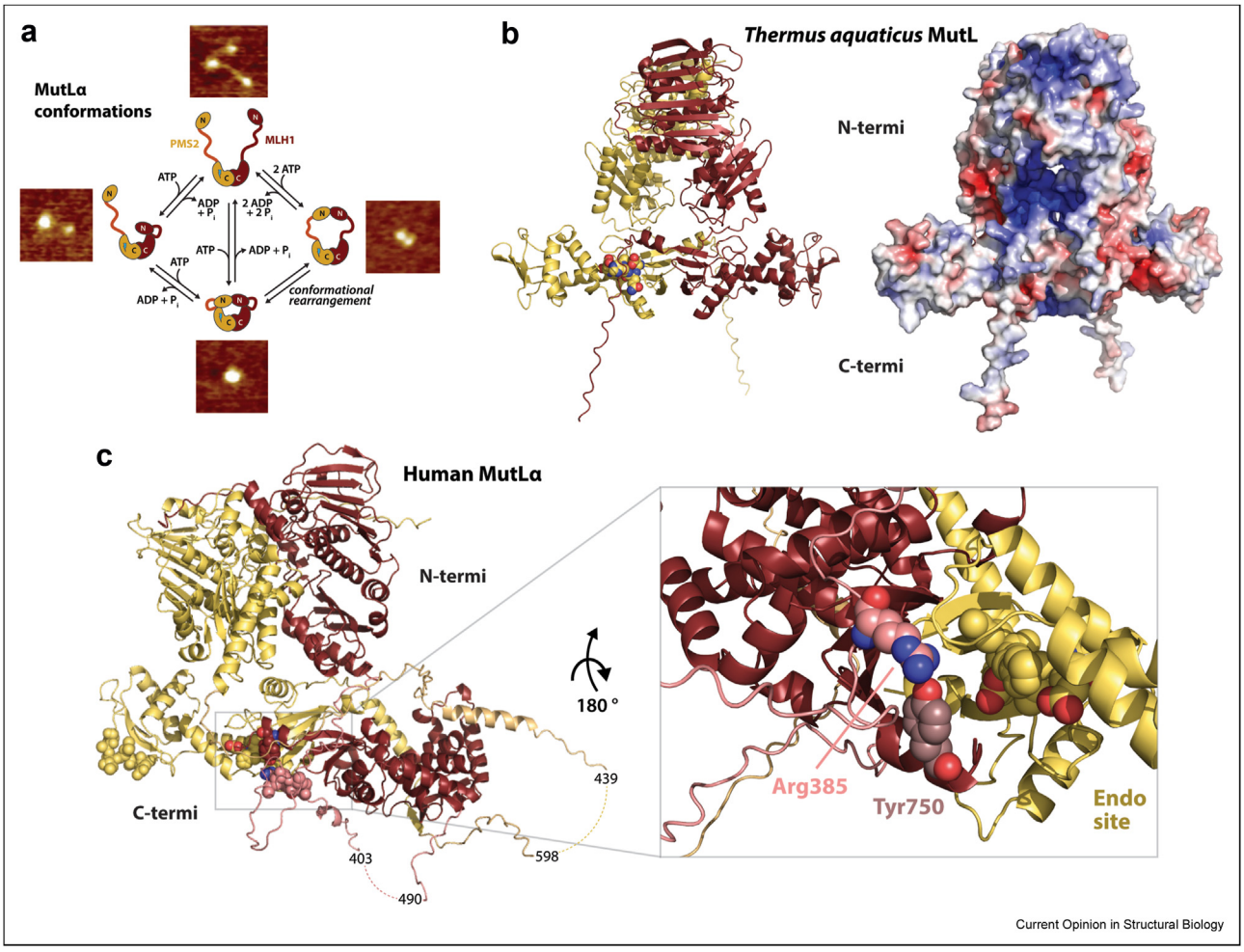

Predicted and observed conformations of MutL(α). (**a**) Cycle of nucleotide-dependent conformational states of MutLα determined by AFM (adapted from Refs. [55,56]). A representative AFM image is shown for each conformation. (**b**) AlphaFold model (left) and electrostatic map (right) of *Taq* MutL showing interactions between the N- and C-terminal domains. The endonuclease site is shown as spheres in one subunit (gold). The electrostatic map shows a positive "pore" (blue) in center where DNA is expected to bind. (**c**) AlphaFold model of human MutLα (from predictome.org) showing interaction between the MLH1 C-terminal domain and a conserved linker arm motif. MLH1 and PMS2 are colored red and gold, respectively. For clarity, disordered residues 404–489 of MLH1 and 440-597 of PMS2 were deleted and replaced by dashed lines. The PCNA binding site is shown as gold spheres. The endonuclease catalytic Glu residues are shown as spheres colored by atom type. The key MLH1 Arg395-MLH1 Tyr550 interaction is shown as spheres, and the zoom shows this interaction and its proximity to the catalytic and PCNA binding sites.

that DNA binding residues of MutL are important for formation and stability of the fast-scanning MutL and its interactions with MutH and UvrD [69]. Biochemical and magnetic tweezers studies provide further evidence that *E. coli* MutL can leave the SL complex by forming a ring around the DNA (via dimerization of N-terminal domains) that can slide along DNA and pass obstacles to reach the hemimethylated dGATC site and activate MutH to nick the unmethylated strand. Subsequently, this *E. coli* MutL-ring interacts with UvrD to facilitate its unwinding of DNA [69,70].

MutLα linker arms contain a conserved motif that brings the N- and C-terminal domains together and is essential for repair

AlphaFold2 models of human MutLα reveal short regions of potential interactions between the linker arms of MLH1 (377–399) and PMS2 (Pms1 in yeast) (415–430; alpha helix) with the C-terminal domains, which bring the N- and C-terminals together (Figure 3c) [67,68] (Predictome.org). Although the majority of residues in the linker regions show poor conservation, these short regions show high evolutionary conservation,

and pathogenic mutations have been identified in both of these conserved motifs [71]. Although there are no data regarding the functional importance of the conserved helix in PMS2, recent studies showed that deletion of the conserved motif in the MLH1 linker abrogates MutLα′s endonuclease and repair activities in yeast and human cell extracts [72,73]. Moving the location of this motif in *Sc*Mlh1 or swapping it from the Mlh1 linker to the *Sc*Pms1 linker maintains repair in yeast, consistent with the linker arms being able to adopt multiple conformations. Interestingly, addition of a 25 amino acid peptide containing this motif to wildtype *Sc*MutLα inhibited nonspecific endonuclease activity, suggesting that interfering with this interaction impairs *Sc*MutLα′s ability to nick DNA [72]. In striking contrast, in human cell extracts, addition of a 32 amino acid peptide containing the conserved motif sequence does not interfere with wildtype MutLα function, and it rescues the MMR defect caused by motif deletion mutants, making it the first example of peptide rescuing a MMR defect caused by a pathogenic mutation *in vitro* [73].

Arg385 in this MLH1 motif is mutated in multiple cancers [72,73], and certain mutations of Arg385 significantly impair repair in *S. cerevisiae in vivo* and in human cell extracts. Based on an AlphaFold structure, Wolf and coworkers speculated that Arg385 may functionally interact with MLH1 Tyr750, which is near the C-terminus (Figure 3C). Mutational analysis confirmed this interaction by swapping the positions of Arg385 and Tyr750 to Tyr385 and Arg750 and showing rescue of the nicking defect caused by mutating Arg 385 [73]. Notably, this interaction is adjacent to the endonuclease active site in the AlphaFold model (Figure 3C), consistent with the effect of mutating Arg385 on impairing MutLα′s nicking activity. This interaction may facilitate bringing the N-terminal domain with DNA bound into the endonuclease site and/or help activate the catalytic activity. Major limitations in our ability to understand the function of MutL(α) are that we have no idea how DNA fits into MutL(α) nor a complete picture of the conformation of the endonuclease site in a catalytically active state. As discussed below, it remains unclear if nicking occurs with one and/or two dsDNAs bound to one MutL(α) [55,74,75].

MutS(α) and MutL(α) form multimeric complexes on mismatch DNA that signal repair

In vivo fluorescence studies in *E. coli* revealed the formation of foci containing multiple MutS and MutL proteins, with more MutL than MutS [23,24]. These results are consistent with early DNA footprinting studies that showed protection of a large region of DNA around the mismatch in the presence of *E. coli* MutS, MutL, and ATP [76,77]. In cells lacking MutH, which stalls the signaling cascade that leads to repair, these foci persisted throughout the cell cycle. Notably, the number of foci directly correlated to the number of mismatches detected by DNA sequencing, suggesting that the foci account for all mismatches [78]. Furthermore, repaired and unrepaired mismatches can be distinguished by foci lifetime, with repaired and unrepaired mismatches having short (∼2 min) and long (∼25 min) lifetimes, respectively. These results taken to together with the *in vitro* data suggest that *E. coli* multimeric SL complexes mark the mismatch and protect from it from being hidden within the nucleoid structure until repair can occur or the cell divides. These *E. coli* SL complexes can release one or more MutL rings to interact with MutH and activate nicking. It remains unclear if MutL(α) forms sliding rings in organisms that utilize non-methyl-directed repair, and they may not be necessary because the non-methyl directed strand discrimination signal (PCNA/β-clamp) is mobile and can travel to the SL complex. *E. coli* MutL and non-methyl-directed MutL homologs have biochemical differences that could impact sliding ring phenomena. Specifically, in non-methyl directed MMR homologs, ATP does not appear to promote dimerization of MutL(α) N-terminal domains and they hydrolyze ATP as monomers [54,56,79]. In addition, the N-terminal domains of *E. coli* MutL preferentially bind single stranded DNA [59]; whereas, the N-terminal domains of MutLα preferentially bind double stranded (ds) DNA, and MutLα can simultaneously bind two dsDNA strands [74,75,79].

In vivo fluorescence studies in *S. cerevisiae* also revealed multimeric SL complexes that contain more *Sc*MutLα than *Sc*MutSα, and foci in wildtype cells showed similar lifetimes (∼2−3 min) to those in *E. coli* [80]. Consistent with these results, single-molecule photobleaching studies of *Taq* proteins and AFM studies of human proteins also show multimeric SL complexes (with 3−8 proteins) on DNA containing a mismatch [16,55]. Using time- and concentration-dependent depositions, the AFM studies further showed that the human SL complexes rearrange, folding and compacting the DNA on the timescale of a few minutes. These results were further confirmed by tethered particle motion experiments [55]. Early AFM studies of *Sc*MutLα in low salt showed that *Sc*MutLα cooperatively binds DNA to form tracts of protein and can bring two DNA molecules together via its N-terminal domains [74]. These results are consistent with the SL complexes being able to reconfigure the DNA. Recent biochemical studies confirm this tethering of DNA molecules and further show that this tethering enhances the endonuclease activity of *Sc*MutLα [75]. These results taken together with the observation from the *Taq* smFRET studies showing MutS can revisit the mismatch suggest that MutS(α) localizes MutL(α) near the mismatch and promotes DNA configurations that could enhance MMR efficiency by facilitating MutL(α) nicking the DNA at

multiple sites around the mismatch. In addition, such complexes may also protect the mismatch region from nucleosome/nucleoid-associated proteins reassembly until repair occurs, and they could potentially remodel adjacent nucleosomes/nucleoid associated proteins [55].

Word of caution: Under physiological conditions, MutL(α) exhibits no significant binding to DNA in the absence of MutS(α) and ATP. Nearly all studies investigating MutL(α)-DNA interactions and nicking in the absence of MutS(α) are conducted in very low monovalent salt concentrations, and for monitoring MutL(α) endonuclease activity, Mg^{++} is replaced with Mn^{++} to increase the nuclease activity.

Unified models of MMR initiation for methyl- and non-methyl-directed repair

The initial steps appear to be well conserved between methyl- and non-methyl-directed MMR; however, the later steps diverge, likely due to the differences in the mechanism of strand discrimination. In *E. coli*, the strand discrimination signal is a static hemimethylated dGATC site; whereas, in non-methyl directed repair, it is PCNA/β-clamp, which is mobile [81]. In *E. coli*, MutL, with or without MutS, must travel to the dGATC site to activate MutH's nicking of the daughter strand. In contrast, PCNA/β-clamp can travel along the DNA to interact with MutL(α) contained within a static or slowly moving SL complex. Taking all the data discussed above together, we present unified models for MMR that take into account the differences in the strand-discrimination signals between methyl- and non-methyl-directed MMR (Figure 4).

During scanning, MutS(α) adopts an array of conformations with different degrees of DNA bending and with Domains I likely down and dynamically interacting with the grooves of the DNA. Upon mismatch recognition, it converts to a state, where the DNA is kinked, with specific interactions between the mismatched base and the conserved Phe and Glu. Subsequently, MutS(α) undergoes a series of ATP-dependent conformational changes, in which Domains I sequentially open and Domains IV cross to form a mobile clamp (Figures 2D and 4). Domain I that is not interacting with the mismatch (SubunitB/MSH2) opens first, which in turn allows MutL(α) to bind while MutS(α) is still at the mismatch. If MutL(α)'s arrival is delayed, the second Domain I disengages the mismatch, such that both Domains I no longer interact with the DNA, and MutS(α) moves away, allowing another MutS(α) to bind the mismatch. In this state, mobile MutS(α) can no longer recognize the mismatch; however, ATP hydrolysis by MutS(α) reengages one or both Domains I with the DNA allowing it to rebind the mismatch (Figure 2C). This rebinding increases the probability that SL complexes are located at or near the mismatch, because movement of MutS(α) clamps is bounded by the replication fork and the reloaded nucleosomes in eukaryotes or nucleoid-associated proteins in bacteria [82]. SL complexes likely form in a stepwise fashion. If MutL(α) stops MutS(α) at the mismatch, more MutL(α) can join the complex until downstream events occur. If MutS(α) moves away from the mismatch before being stopped by MutL(α), another MutS(α) can bind the mismatch to form an additional clamp that can interact with the existing SL complex and/or recruit more MutL(α) (Figure 4). Notably, these complexes appear to be dynamic with MutL(α) joining and leaving and MutS(α) undergoing conformational changes [16,55]. These complexes may serve to mark and protect the mismatch until repair can occur.

In *E. coli*, if these SL complexes are sufficiently close to a hemimethylated dGATC site, MutL within the SL complex can activate MutH to nick the daughter strand. Alternatively, MutL can form a ring around the DNA that can leave the SL complex and rapidly move along DNA (Figure 4). MutH can join and travel with these MutL-rings to the hemimethylated dGATC site and nick the unmethylated daughter strand. Subsequently, this MutL-ring can activate UvrD to unwind the DNA, allowing single-stranded exonucleases to excise the mismatch, which can be up to 1000 bp from the dGATC site. Although the signal to terminate excision is unknown, the multimeric SL complexes that remain at the mismatch [78] may get displaced via the MutL-UvrD-exonuclease activity, and their displacment after the mismatch has been removed may provide the signal to terminate excision. This suggestion is consistent with the observation that multimeric SL complexes remain through cell division in cells in which MutH is deleted [78]. Finally, after mismatch excision, DNA polymerase III fills in the gap and DNA ligase seals the nick, completing repair.

In non-methyl-directed repair, there is no need for MutL(α) to leave the SL complex, and currently there is no that evidence that MutL(α) leaves an SL complex as a fast moving mobile ring. Instead, the SL complexes appear to assemble "linearly" along the DNA and, over time, evolve to more globular forms that can reconfigure the DNA. This reconfiguration involves compaction of DNA within the protein complexes and, in some cases, loop formation [55]. MutLα′s abilities to simultaneously interact with two double strands of DNA via its N-terminal domains [60,74,79] and to undergo large ATP-induced conformational changes (Figure 3A) [56] may promote this compaction. For example, DNA reconfiguration will result if one of the MutLα N-terminal domains binds distally on the DNA with that arm in an extended state (as in Figure 4), followed by nucleotide-induced retraction of that arm toward the C-terminal domains containing the endonuclease site (Figures 3 and 4). This process is stochastic, and the location on

Figure 4

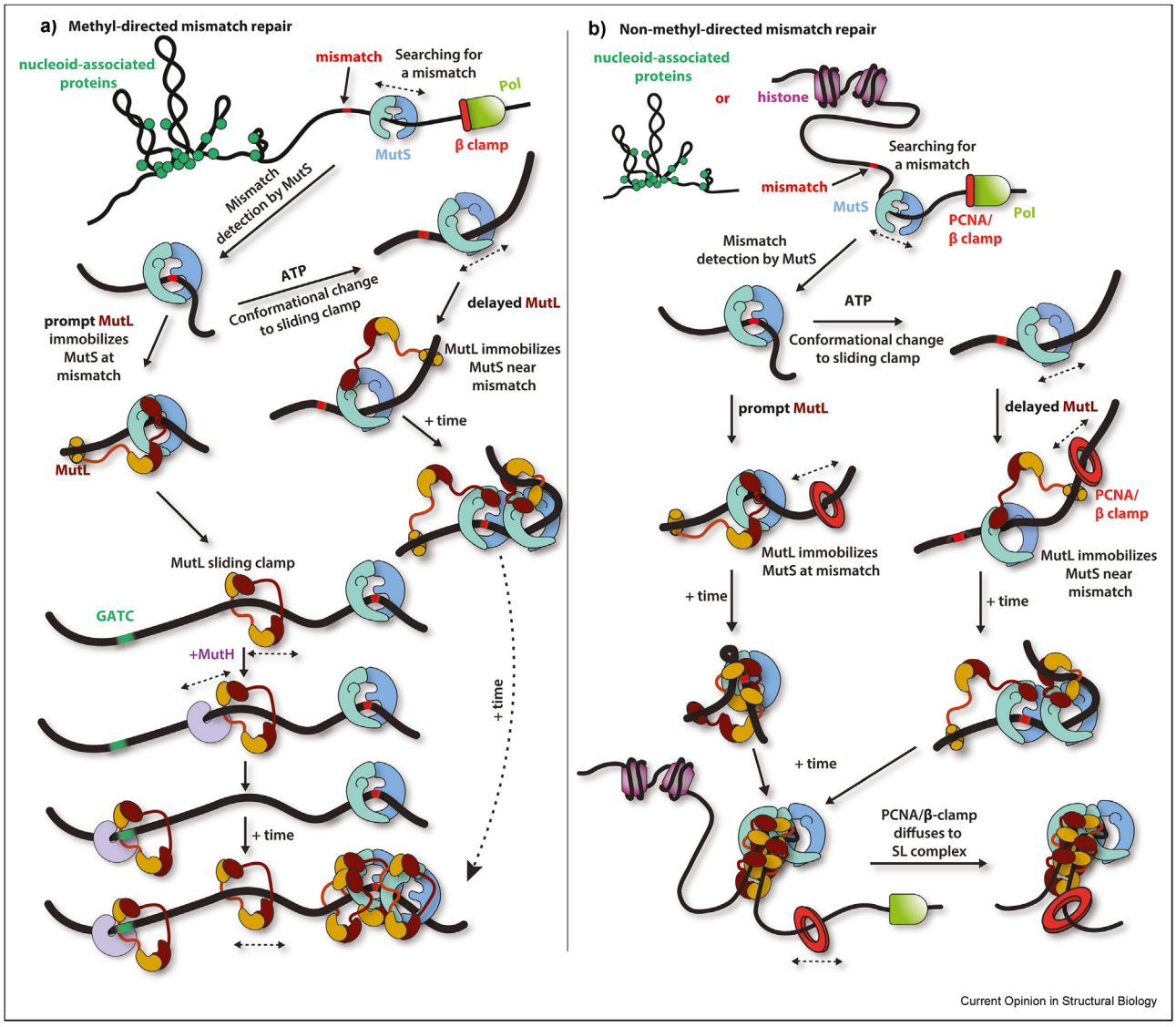

Unified models of MMR for methyl- and non-methyl-directed MMR. Both methyl- and non-methyl-directed MMR (**a**, **b**) begin by MutS(α) searching the DNA between the replication fork and the reloaded nucleoid-associated proteins in bacteria or nucleosomes in eukaryotes until it locates and binds a mismatch (**a**, **b**, top). After recognition, MutS(α) undergoes ATP-dependent conformational changes that result in the interaction with MutL(α), or MutS(α) undergoes further conformational changes to form a mobile clamp that moves away from the mismatch, where MutL(α) can trap it. Additional MutS(α) can load on the mismatch and additional MutL(α) can join MutS(α) at or away from the mismatch. At this point, the mechanism of methyl- and non-methyl-directed MMR diverge. For methyl-directed MMR (**a**), the MutL proteins loaded on DNA by MutS can form rings around the DNA and depart MutS, rapidly scanning the DNA. MutH can join the MutL-ring, and they travel together to the hemimethylated dGATC site. If repair does not occur, multimeric MuS−MutL complexes remain associated with the mismatch. In non-methyl-directed repair (**b**), PCNA/β-clamp can slide away from the replication fork to activate MutL(α) to nick the daughter strand in any of the SL complexes. If downstream repair proteins are delayed, additional MutL(α) (and MutS(α)) proteins can join the complex and subsequently rearrange and compact the DNA. Dashed double-headed arrows indicate a diffusing complex. In **b**, PCNA/β-clamp is only shown in some cartoons for simplicity

the DNA where the MutLα N-terminal domain binds will determine the details of the final compacted state. MutSα may also contribute to the DNA reconfiguration, given that MutS(α) remains dynamic in SL complexes [16], and ATP-activated MutSα can self-associate on mismatch containing DNA [55]. Subsequent interaction of PCNA/β-clamp with MutL(α) activates its endonuclease activity to nick the daughter strand locally to the mismatch, thereby allowing excision and repair to commence. Any SL complex, including a single MutS(α)-MutL(α) complex (or even a single MutL(α) that has been loaded onto the DNA by MutS(α)), should be competent for activation by PCNA [13,31,83].

If the arrival of downstream repair proteins, such as PCNA/β-clamp, is delayed, the SL complexes may continue to reorganize and compact DNA within the complex [55] (Figure 4). These dynamic SL assemblies on the naked DNA between the replication fork and nucleosomes/nucleoid associated proteins could have multiple functions. *i*) They could prevent nucleosome/nucleoid associated protein assembly over mismatch-containing DNA or possibly move these proteins off the mismatch. Recent studies showing that active MMR preferentially inhibits nucleosome loading near mismatches support this idea [84,85]. *ii*) Long-lived SL complexes at or near the mismatch also may mark and protect the mismatch until repair can proceed. *iii*) Folding of DNA by SL complexes could facilitate MutLα nicking the daughter strand on both sides of the mismatch [30,31] by generating antiparallel double-stranded DNA configurations that bring PCNA/β-clamp in proximity to both sides [13] (Figure 4). *iv*) The dynamic rearrangement of mismatch DNA by SL complexes could promote multiple MutLα-induced nicks around the mismatch [13,30]. These multiple nicks should facilitate the next stage of DNA repair by providing multiple entry points for EXO1 or a strand-displacing polymerase [4,30]. *v*) Finally, the dissolution of the SL complex as the daughter strand is excised past the mismatch could signal the end of excision.

Conclusions and open questions

The recent studies have clarified the mechanisms of MMR initiation pathways from MutS(α) searching and mismatch recognition to recruitment of MutL(α) and MutL(α)'s subsequent interaction with the strand discrimination signal. Although these recent results have also given deep insights into the conformational changes in MutS(α), MutL(α), and mismatched DNA during MMR initiation, major questions remain. Despite the wealth of knowledge that we have gained about MutS(α) conformational transitions, we still lack understanding of nucleotide occupancies that coordinate these transitions. We have comparatively little mechanistic understanding of MutL(α). Due to the flexibility of MutL(α)'s linker arms, we lack an understanding of its functional conformations or the nature of its interactions within SL complexes. Significantly, we do not know where the DNA is located in MutL(α) or SL complexes, how MutL activates MutH's endonuclease activity in *E. coli*, or how ATP and PCNA/β-clamp activate MutL(α)'s nicking activity in non-methyl-directed repair. Finally, despite having a crystal structure of interaction of the *Bacillus subtilis* β-clamp bound to a fragment of MutL C-terminal domain [86], we lack insight into how β-clamp (or PCNA) directs nicking to the daughter strand.

Declaration of competing interest

The authors declare that they have no known competing financial interests or personal relationships that could have appeared to influence the work reported in this paper.

Data availability

No data was used for the research described in the article.

Acknowledgements

We are grateful to Caitlin Johnson for making all the figures. We would like to thank Sharonda LeBlanc and Caitlin Johnson for critically reading the manuscript. This research funded by National Institute of General Medical Sciences grants R35 GM127151 (to D.A.E.), R01 GM132263 (to K.R.W.) and the National Science Foundation grant MCB-2409309 to K.R.W.

References

Papers of particular interest, published within the period of review, have been highlighted as:

- • of special interest
- •• of outstanding interest

1. Kunkel TA, Erie DA: **DNA mismatch repair**. *Annu Rev Biochem* 2005, **74**:681–710.
2. Iyer RR, Pluciennik A, Burdett V, Modrich PL: **DNA mismatch repair: functions and mechanisms**. *Chem Rev* 2006, **106**: 302–323.
3. Hsieh P, Yamane K: **DNA mismatch repair: molecular mechanism, cancer, and ageing**. *Mech Ageing Dev* 2008, **129**: 391–407.
4. Modrich P: **Mechanisms in E. coli and human mismatch repair (Nobel Lecture)**. *Angew Chem Int Ed Engl* 2016, **55**:8490–8501.
5. Chakraborty U, Alani E: **Understanding how mismatch repair proteins participate in the repair/anti-recombination decision**. *FEMS Yeast Res* 2016, **16**. fow071.
6. Mendillo ML, Putnam CD, Kolodner RD: **Escherichia coli MutS tetramerization domain structure reveals that stable dimers but not tetramers are essential for DNA mismatch repair in vivo**. *J Biol Chem* 2007, **282**:16345–16354.
7. Calmann MA, Nowosielska A, Marinus MG: **Separation of mutation avoidance and antirecombination functions in an Escherichia coli mutS mutant**. *Nucleic Acids Res* 2005, **33**: 1193–1200.
8. Bjornson KP, Blackwell LJ, Sage H, Baitinger C, Allen D, Modrich P: **Assembly and molecular activities of the MutS tetramer**. *J Biol Chem* 2003, **278**:34667–34673.
9. Takamatsu S, Kato R, Kuramitsu S: **Mismatch DNA recognition protein from an extremely thermophilic bacterium, Thermus thermophilus HB8**. *Nucleic Acids Res* 1996, **24**:640–647.
10. Biswas I, Ban C, Fleming KG, Qin J, Lary JW, Yphantis DA, Yang W, Hsieh P: **Oligomerization of a MutS mismatch repair protein from Thermus aquaticus**. *J Biol Chem* 1999, **274**: 23673–23678.
11. Miguel V, Monti MR, Argarana CE: **The role of MutS oligomers on Pseudomonas aeruginosa mismatch repair system activity**. *DNA Repair* 2008, **7**:1799–1808.
12. Gradia S, Subramanian D, Wilson T, Acharya S, Makhov A, Griffith J, Fishel R: **hMSH2-hMSH6 forms a hydrolysis-independent sliding clamp on mismatched DNA**. *Mol Cell* 1999, **3**:255–261.
13. Kunkel TA, Erie DA: **Eukaryotic mismatch repair in relation to DNA replication**. *Annu Rev Genet* 2015, **49**:291–313.

14. Reyes GX, Schmidt TT, Kolodner RD, Hombauer H: **New insights into the mechanism of DNA mismatch repair**. *Chromosoma* 2015, **124**:443–462.

15. Qiu R, DeRocco VC, Harris C, Sharma A, Hingorani MM, Erie DA, Weninger KR: **Large conformational changes in MutS during DNA scanning, mismatch recognition and repair signalling**. *EMBO J* 2012, **31**:2528–2540.

16. Qiu R, Sakato M, Sacho EJ, Wilkins H, Zhang X, Modrich P, Hingorani MM, Erie DA, Weninger KR: **MutL traps MutS at a DNA mismatch**. *Proc Natl Acad Sci U S A* 2015, **112**: 10914–10919.

17. LeBlanc SJ, Gauer JW, Hao P, Case BC, Hingorani MM, Weninger KR, Erie DA: **Coordinated protein and DNA conformational changes govern mismatch repair initiation by MutS**. *Nucleic Acids Res* 2018, **46**:10782–10795.

18. Groothuizen FS, Winkler I, Cristóvão M, Fish A: **MutS/MutL crystal structure reveals that the MutS sliding clamp loads MutL onto DNA**. *eLife* 2015, **4**, e06744.

19. Jeong C, Cho WK, Song KM, Cook C, Yoon TY, Ban C, Fishel R, Lee JB: **MutS switches between two fundamentally distinct clamps during mismatch repair**. *Nat Struct Mol Biol* 2011, **18**: 379–385.

20. Liu J, Hanne J, Britton BM, Bennett J, Kim D, Lee JB, Fishel R: **Cascading MutS and MutL sliding clamps control DNA diffusion to activate mismatch repair**. *Nature* 2016, **539**: 583–587.

21. Mendillo ML, Putnam CD, Mo AO, Jamison JW, Li S, Woods Jr VL, Kolodner RD: **Probing DNA- and ATP-mediated conformational changes in the MutS family of mispair recognition proteins using deuterium exchange mass spectrometry**. *J Biol Chem* 2010, **285**:13170–13182.

22. Josephs EA, Zheng T, Marszalek PE: **Atomic force microscopy captures the initiation of methyl-directed DNA mismatch repair**. *DNA Repair* 2015, **35**:71–84. Elsevier B.V.

23. Elez M, Murray AW, Bi LJ, Zhang XE, Matic I, Radman M: **Seeing mutations in living cells**. *Curr Biol* 2010, **20**:1432–1437.

24. Elez M, Radman M, Matic I: **Stoichiometry of MutS and MutL at unrepaired mismatches in vivo suggests a mechanism of repair**. *Nucleic Acids Res* 2012, **40**:3929–3938.

25. Martin-Lopez JV, Fishel R: **The mechanism of mismatch repair and the functional analysis of mismatch repair defects in Lynch syndrome**. *Fam Cancer* 2013, **12**:159–168.

26. Boland CR, Lynch HT: **The history of Lynch syndrome**. *Fam Cancer* 2013, **12**:145–157.

27. Heinen CD: **Mismatch repair defects and Lynch syndrome: the role of the basic scientist in the battle against cancer**. *DNA Repair* 2016, **38**:127–134.

28. Lebbink JH, Drost M, de Wind N: **DNA mismatch repair: from biophysics to bedside**. *DNA Repair* 2016, **38**:1–2.

29. Putnam CD: **Evolution of the methyl directed mismatch repair system in Escherichia coli**. *DNA Repair* 2016, **38**:32–41.

30. Kadyrov FA, Dzantiev L, Constantin N, Modrich P: **Endonucleolytic function of MutLalpha in human mismatch repair**. *Cell* 2006, **126**:297–308.

31. Kadyrov FA, Holmes SF, Arana ME, Lukianova OA, O'Donnell M, Kunkel TA, Modrich P: **Saccharomyces cerevisiae MutLa is a mismatch repair endonuclease**. *J Biol Chem* 2007, **282**: 37181–37190.

32. Smith CE, Mendillo ML, Bowen N, Hombauer H, Campbell CS, Desai A, Putnam CD, Kolodner RD: **Dominant mutations in S. cerevisiae PMS1 identify the Mlh1-Pms1 endonuclease active site and an exonuclease 1-independent mismatch repair pathway**. *PLoS Genet* 2013, **9**, e1003869.

33. Lamers MH, Perrakis A, Enzlin JH, Winterwerp HH, de Wind N, Sixma TK: **The crystal structure of DNA mismatch repair protein MutS binding to a G x T mismatch**. *Nature* 2000, **407**: 711–717.

34. Obmolova G, Ban C, Hsieh P, Yang W: **Crystal structures of mismatch repair protein MutS and its complex with a substrate DNA**. *Nature* 2000, **407**:703–710.

35. Natrajan G, Lamers MH, Enzlin JH, Winterwerp HH, Perrakis A, Sixma TK: **Structures of Escherichia coli DNA mismatch repair enzyme MutS in complex with different mismatches: a common recognition mode for diverse substrates**. *Nucleic Acids Res* 2003, **31**:4814–4821.

36. Warren JJ, Pohlhaus TJ, Changela A, Iyer RR, Modrich PL, Beese LS: **Structure of the human MutSalpha DNA lesion recognition complex**. *Mol Cell* 2007, **26**:579–592.

37. Bruekner SR, Pieters W, Fish A, Liaci AM, Scheffers S, Rayner E, Kaldenbach D, Drost L, Dekker M, van Hees-Stuivenberg S, *et al.*: **Unexpected moves: a conformational change in MutSα enables high-affinity DNA mismatch binding**. *Nucleic Acids Res* 2023, **51**:1173–1188.

38. • Borsellini A, Kunetsky V, Friedhoff P, Lamers MH: **Cryogenic electron microscopy structures reveal how ATP and DNA binding in MutS coordinates sequential steps of DNA mismatch repair**. *Nat Struct Mol Biol* 2022, **29**:59–66.
Cryo-EM and FRET are used to determine structures of *E. coli* MutS in 4 nucleotide-liganded states representing steps in its ATP hydrolysis pathway. Large conformational differences are characterized. Combined with other studies, the authors provide insight into how ATP hydrolysis and DNA interactions combine to help coordinate the stepwise path of conformational dynamics when MutS recognizes mismatches.

39. Nirwal S, Kulkarni DS, Sharma A, Rao DN, Nair DT: **Mechanism of formation of a toroid around DNA by the mismatch sensor protein**. *Nucleic Acids Res* 2018, **46**:256–266.

40. Lee J-H, Thomsen M, Daub H, Steinbacher SC, Sztyler A, Thieulin-Pardo G, Neudegger T, Plotnikov NV, Iyer RR, Wilkinson HA, *et al.*: **Conformational dynamics and DNA recognition by human MutSβ**. *bioRxiv* 2023. 2023.2005.2008.539930.

41. • Jayaraj A, Thayer KM, Beveridge DL, Hingorani MM: **Molecular dynamics of mismatch detection—how MutS uses indirect readout to find errors in DNA**. *Biophys J* 2023, **122**:3031–3043.
All atom molecular dynamics is applied to study the conformational dynamics of *T. aquaticus* MutS in a searching mode. The DNA in the mismatch-bound crystal structure is converted to duplex DNA and then the dynamics of the complex are followed for 10 μs. A stepwise sequence of MutS conformational transitions and DNA bending/unbending is characterized that represents the transition from MutS searching to mismatch recognition.

42. Inoue K, Takada S, Terakawa T: **Coarse-grained molecular dynamics simulations of base-pair mismatch recognition protein MutS sliding along DNA**. *Biophysics and Physicobiology* 2022, **19**. n/a.

43. Wang H, Yang Y, Schofield MJ, Du C, Fridman Y, Lee SD, Larson ED, Drummond JT, Alani E, Hsieh P, *et al.*: **DNA bending and unbending by MutS govern mismatch recognition and specificity**. *Proc Natl Acad Sci U S A* 2003, **100**:14822–14827.

44. Tessmer I, Yang Y, Zhai J, Du C, Hsieh P, Hingorani MM, Erie DA: **Mechanism of MutS searching for DNA mismatches and signaling repair**. *J Biol Chem* 2008, **283**:36646–36654.

45. Gorman J, Chowdhury A, Surtees JA, Shimada J, Reichman DR, Alani E, Greene EC: **Dynamic basis for one-dimensional DNA scanning by the mismatch repair complex Msh2-Msh6**. *Mol Cell* 2007, **28**:359–370.

46. Cho W-K, Jeong C, Kim D, Chang M, Song K-M, Hanne J, Ban C, Fishel R, Lee J-B: **ATP alters the diffusion mechanics of MutS on mismatched DNA**. *Structure* 2012, **20**:1264–1274.

47. Sass LE, Lanyi C, Weninger K, Erie DA: **Single-molecule FRET TACKLE reveals highly dynamic mismatched DNA-MutS complexes**. *Biochemistry* 2010, **49**:3174–3190.

48. DeRocco VC, Sass LE, Qiu R, Weninger KR, Erie DA: **Dynamics of MutS–mismatched DNA complexes are predictive of their repair phenotypes**. *Biochemistry* 2014, **53**:2043–2052.

49. •• Hao P, LeBlanc SJ, Case BC, Elston TC, Hingorani MM, Erie DA, Weninger KR: **Recurrent mismatch binding by MutS mobile**

clamps on DNA localizes repair complexes nearby *Proc Nat Acad Sci* 2020, **117**:17775–17784.
Using smFRET measurements of *Taq* MutS and MutL, this study demonstrates that after the ATP and mismatch dependent formation of a MutS mobile clamp, ATP hydrolysis allows it to convert to state that can rebind the mismatch. MutL is shown to be able to bind the MutS sliding clamp and stop its movement. These measurements, combined with other results allow determination of the free energy landscape governing the interactions of MutS with a mismatch from recognition to mobile clamp transition and back to rebind the mismatch.

50. Guarne A, Ramon-Maiques S, Wolff EM, Ghirlando R, Hu X, Miller JH, Yang W: **Structure of the MutL C-terminal domain: a model of intact MutL and its roles in mismatch repair**. *EMBO J* 2004, **23**:4134–4145.

51. Guarné A, Charbonnier JB: **Insights from a decade of biophysical studies on MutL: roles in strand discrimination and mismatch removal**. *Prog Biophys Mol Biol* 2015, **117**:149–156.

52. • Fernandez-Leiro R, Bhairosing-Kok D, Kunetsky V, Laffeber C, Winterwerp HH, Groothuizen F, Fish A, Lebbink JHG, Friedhoff P, Sixma TK, *et al.*: **The selection process of licensing a DNA mismatch for repair**. *Nat Struct Mol Biol* 2021, **28**:373–381.
In this study, they determined the cryo-EM structures of *E. coli* MutS bound to homoduplex DNA and in several conformations on mismatch DNA: mismatch bound, intermediates on the transition to a mobile clamp, a mobile clamp, and a MutL N-terminal domain bound state. These structures reveal details of conformational changes that occur across the spectrum of MutS MMR functions. Notably, evidence is presented for variable degrees of DNA bending during the searching phase.

53. Fukui K, Baba S, Kumasaka T, Yano T: **Structural features and functional dependency on β-clamp define distinct subfamilies of bacterial mismatch repair endonuclease MutL**. *J Biol Chem* 2016, **291**:16990–17000.

54. Gueneau E, Dherin C, Legrand P, Tellier-Lebegue C, Gilquin B, Bonnesoeur P, Londino F, Quemener C, Le Du MH, Marquez JA, *et al.*: **Structure of the MutLalpha C-terminal domain reveals how Mlh1 contributes to Pms1 endonuclease site**. *Nat Struct Mol Biol* 2013, **20**:461–468.

55. •• Bradford KC, Wilkins H, Hao P, Li ZM, Wang B, Burke D, Wu D, Smith AE, Spaller L, Du C, *et al.*: **Dynamic human MutSα–MutLα complexes compact mismatched DNA**. *Proc Natl Acad Sci USA* 2020, **117**:16302–16312.
This study used AFM imaging to reveal time and concentration dependence of complexes of human MutSα and MutLα that assemble on mismatched DNA. They found surprising stoichiometries and conformations with 3–8 proteins assembling in complexes that compacted DNA. This surprising behavior is suggested to enable multiple MutLα nicking hear the mismatch and to protect the mismatch area from reloading nucleosomes if repair is not sufficiently prompt.

56. Sacho EJ, Kadyrov FA, Modrich P, Kunkel TA, Erie DA: **Direct visualization of asymmetric adenine-nucleotide-induced conformational changes in MutL alpha**. *Mol Cell* 2008, **29**:112–121.

57. Pang Q, Prolla TA, Liskay RM: **Functional domains of the Saccharomyces cerevisiae Mlh1p and Pms1p DNA mismatch repair proteins and their relevance to human hereditary nonpolyposis colorectal cancer-associated mutations**. *Mol Cell Biol* 1997, **17**:4465–4473.

58. Tran PT, Liskay RM: **Functional studies on the candidate ATPase domains of Saccharomyces cerevisiae MutLalpha**. *Mol Cell Biol* 2000, **20**:6390–6398.

59. Ban C, Junop M, Yang W: **Transformation of MutL by ATP binding and hydrolysis: a switch in DNA mismatch repair**. *Cell* 1999, **97**:85–97.

60. Hall MC, Shcherbakova PV, Kunkel TA: **Differential ATP binding and intrinsic ATP hydrolysis by amino-terminal domains of the yeast Mlh1 and Pms1 proteins**. *J Biol Chem* 2002, **277**:3673–3679.

61. Groothuizen FS, Sixma TK: **The conserved molecular machinery in DNA mismatch repair enzyme structures**. *DNA Repair* 2016, **38**:14–23.

62. Pillon MC, Lorenowicz JJ, Uckelmann M, Klocko AD, Mitchell RR, Chung YS, Modrich P, Walker GC, Simmons LA, Friedhoff P, *et al.*: **Structure of the endonuclease domain of MutL: unlicensed to cut**. *Mol Cell* 2010, **39**:145–151.

63. Pillon MC, Babu VM, Randall JR, Cai J, Simmons LA, Sutton MD, Guarne A: **The sliding clamp tethers the endonuclease domain of MutL to DNA**. *Nucleic Acids Res* 2015, **43**:10746–10759.

64. Pillon MC, Miller JH, Guarne A: **The endonuclease domain of MutL interacts with the beta sliding clamp**. *DNA Repair* 2011, **10**:87–93.

65. Mendillo ML, Hargreaves VV, Jamison JW, Mo AO, Li S, Putnam CD, Woods Jr VL, Kolodner RD: **A conserved MutS homolog connector domain interface interacts with MutL homologs**. *Proc Natl Acad Sci U S A* 2009, **106**:22223–22228.

66. Jumper J, Evans R, Pritzel A, Green T, Figurnov M, Ronneberger O, Tunyasuvunakool K, Bates R, Žídek A, Potapenko A, *et al.*: **Highly accurate protein structure prediction with AlphaFold**. *Nature* 2021, **596**:583–589.

67. Evans R, O'Neill M, Pritzel A, Antropova N, Senior A, Green T, Žídek A, Bates R, Blackwell S, Yim J, *et al.*: **Protein complex prediction with AlphaFold-Multimer**. *bioRxiv* 2022. 2021.2010.2004.463034.

68. Mirdita M, Schütze K, Moriwaki Y, Heo L, Ovchinnikov S, Steinegger M: **ColabFold: making protein folding accessible to all**. *Nat Methods* 2022, **19**:679–682.

69. •• Yang X-W, Han X-P, Han C, London J, Fishel R, Liu J: **MutS functions as a clamp loader by positioning MutL on the DNA during mismatch repair**. *Nat Commun* 2022, **13**:5808.
This study applies single molecule fluorescence methods to characterize *E. coli* MMR proteins moving long distances along stretched DNA. Interactions among MutS, MutL, MutH and UvrD were characterized. This study demonstrates requirements to load sliding MutL-rings on DNA, the impact of a positively charged patch in the MutL N-terminal domain on the mobility of the MutL-ring, and the ability of MutL-rings to promote MutH and UvrD activities.

70. Mardenborough YSN, Nitsenko K, Laffeber C, Duboc C, Sahin E, Quessada-Vial A, Winterwerp HHK, Sixma TK, Kanaar R, Friedhoff P, *et al.*: **The unstructured linker arms of MutL enable GATC site incision beyond roadblocks during initiation of DNA mismatch repair**. *Nucleic Acids Res* 2019, **47**:11667–11680.

71. The UniProt Consortium: **UniProt: the universal protein knowledgeable**. *Nucleic Acids Res* 2016, **45**:D158–D169.

72. • Torres KA, Calil FA, Zhou AL, DuPrie ML, Putnam CD, Kolodner RD: **The unstructured linker of Mlh1 contains a motif required for endonuclease function which is mutated in cancers**. *Proc Natl Acad Sci USA* 2022, **119**, e2212870119.
This study demonstrates that a short, conserved motif in the linker region of Mlh1 is required for MMR in yeast. They demonstrate that MMR is supported with the motif moved within the Mlh1 linker and when swapped to the Pms1 linker. Mutations in the linker motif increase MutLα foci in yeast cells and are found in multiple human cancer-associated variants.

73. • Wolf K, Kosinski J, Gibson TJ, Wesch N, Dötsch V, Genuardi M, Cordisco EL, Zeuzem S, Brieger A, Plotz G: **A conserved motif in the disordered linker of human MLH1 is vital for DNA mismatch repair and its function is diminished by a cancer family mutation**. *Nucleic Acids Res* 2023, **51**:6307–6320.
This study identified a small motif in the human MLH1 linker domain of MutLα that is highly conserved in eukaryotes, essential for MMR activity, and pathogenic when mutated. An AlphaFold model suggested the importance of a specific interaction of the linker motif with the C-terminal domain near the endonuclease site that was experimentally confirmed to be essential for MMR. MMR defects caused by mutation in this conserved motif could be rescued by addition of a short peptide containing the motif.

74. Hall MC, Wang H, Erie DA, Kunkel TA: **High affinity cooperative DNA binding by the yeast Mlh1-Pms1 heterodimer**. *J Mol Biol* 2001, **312**:637–647.

75. Witte Scott J, Rosa Isabella M, Collingwood Bryce W, Piscitelli Jonathan M, Manhart Carol M: **The mismatch repair endonuclease MutLα tethers duplex regions of DNA together and**

relieves DNA torsional tension. *Nucleic Acids Res* 2023, **51**: 2725–2739.

76. Selmane T, Schofield MJ, Nayak S, Du C, Hsieh P: **Formation of a DNA mismatch repair complex mediated by ATP**. *J Mol Biol* 2003, **334**:949–965.

77. Grilley M, Welsh KM, Su SS, Modrich P: **Isolation and characterization of the Escherichia coli mutL gene product**. *J Biol Chem* 1989, **264**:1000–1004.

78. •• Enrico Bena C, Ollion J, De Paepe M, Ventroux M, Robert L, Elez M: **Real-time monitoring of replication errors' fate reveals the origin and dynamics of spontaneous mutations**. *Nat Commun* 2024, **15**:2702–2712.
This study used a novel microfluidic device to image MMR protein foci via fluorescently tagged MutL in individual *E. coli* cells over multiple cell cycles. They found both short- and long-lived foci, with the foci lifetime being dependent on the MutH and DNA adenine methylase (Dam) levels. They correlated foci behaviors with mismatch fates using whole genome sequencing. The short and long lifetimes of MMR protein foci were associated with repaired and unrepaired mismatch errors respectively. Sub-populations of cells were identified that show cell-to-cell variability in mismatch repair capacity.

79. Hall MC, Shcherbakova PV, Fortune JM, Borchers CH, Dial JM, Tomer KB, Kunkel TA: **DNA binding by yeast Mlh1 and Pms1: implications for DNA mismatch repair**. *Nucleic Acids Res* 2003, **31**:2025–2034.

80. Hombauer H, Campbell CS, Smith CE, Desai A, Kolodner RD: **Visualization of eukaryotic DNA mismatch repair reveals distinct recognition and repair intermediates**. *Cell* 2011, **147**: 1040–1053.

81. Kochaniak AB, Habuchi S, Loparo JJ, Chang DJ, Cimprich KA, Walter JC, van Oijen AM: **Proliferating cell nuclear antigen uses two distinct modes to move along DNA**. *J Biol Chem* 2009, **284**:17700–17710.

82. Wang X, Montero Llopis P, Rudner DZ: **Organization and segregation of bacterial chromosomes**. *Nat Rev Genet* 2013, **14**:191–203.

83. Genschel J, Kadyrova LY, Iyer RR, Dahal BK, Kadyrov FA, Modrich P: **Interaction of proliferating cell nuclear antigen with PMS2 is required for MutLalpha activation and function in mismatch repair**. *Proc Natl Acad Sci U S A* 2017, **114**: 4930–4935.

84. Schopf B, Bregenhorn S, Quivy JP, Kadyrov FA, Almouzni G, Jiricny J: **Interplay between mismatch repair and chromatin assembly**. *Proc Natl Acad Sci U S A* 2012, **109**: 1895–1900.

85. Rodriges Blanko E, Kadyrova LY, Kadyrov FA: **DNA mismatch repair interacts with CAF-1- and ASF1A-H3-H4-dependent histone (H3-H4)2 tetramer deposition**. *J Biol Chem* 2016, **291**: 9203–9217.

86. Almawi AW, Scotland MK, Randall JR, Liu L, Martin HK, Sacre L, Shen Y, Pillon MC, Simmons LA, Sutton MD, *et al.*: **Binding of the regulatory domain of MutL to the sliding beta-clamp is species specific**. *Nucleic Acids Res* 2019, **47**: 4831–4842.